

# TEXTURE-AWARE SUPERPIXEL SEGMENTATION

Rémi Giraud<sup>1</sup> Vinh-Thong Ta<sup>2</sup> Nicolas Papadakis<sup>3</sup> Yannick Berthoumieu<sup>1</sup>

<sup>1</sup>Univ. Bordeaux, Bordeaux INP, IMS, CNRS, UMR 5218, F-33400 Talence, France.

<sup>2</sup>Univ. Bordeaux, Bordeaux INP, LaBRI, CNRS, UMR 5800, F-33400 Talence, France.

<sup>3</sup>Univ. Bordeaux, IMB, CNRS, UMR 5251, F-33400 Talence, France.

## ABSTRACT

Most superpixel methods are based on spatial and color measures at the pixel level. Therefore, they can highly fail to group pixels with similar local texture properties, and need fine parameter tuning to balance the two measures. In this paper, we address these issues with a new Texture-Aware SuperPixel (TASP) segmentation method. TASP locally adjusts its spatial regularity constraint according to the feature variance to accurately segment both smooth and textured areas. A new pixel to superpixel patch-based distance is also proposed to ensure texture homogeneity within created regions. TASP substantially outperforms the segmentation accuracy of state-of-the-art methods on both natural color and texture images.

**Index Terms**— Superpixels, Texture, Patch, Segmentation

## 1. INTRODUCTION

Superpixel segmentation approaches that locally group pixels into regions have become very popular in image processing and computer vision applications. The aim is to exploit the local redundancy of information to lower the computational burden and to potentially improve the performances by reducing the noise of a pixel-wise processing. Superpixels can also be considered as a multi-resolution approach that preserves image contours, contrary to standard regular downsampling methods. It is thus a very interesting pre-processing for applications such as visual saliency estimation [1, 2], data association across views [3], segmentation and classification [4, 5, 6] and object detection [7, 8, 9] or tracking [10, 11].

For the past years, most superpixel methods have tended to produce equally-sized regions containing homogeneous pixels in terms of color. This paradigm is usually in line with the segmentation of an image objects, whose contours can be detected by color changes. Hence, to cluster the pixels into regions, state-of-the-art methods such as [12, 13, 14, 15, 16], only use distance terms in spatial and color (*e.g.*, CIELab) spaces. In [17, 18], more advanced feature spaces are defined to improve the segmentation performances. More recently, [19] proposes to consider contour information in the clustering to ensure the respect of the object boundaries. Never-

theless, such framework requires the need for prior contour detection, at the expense of a global higher complexity.

Most of these state-of-the-art methods only use the pixel color information as clustering feature. Therefore, they can be severely impacted by high contrast variations and fail to produce equally-sized regions having the same textural properties. The proposed method TASP is compared in Figure 1 to the state-of-the-art ones on a synthetic texture image. While TASP produces a relevant segmentation, all other methods are highly misled by the texture patterns. We used the regularity parameters recommended by the authors for tunable methods [14, 15, 20, 18, 19], but no other setting would enable to capture texture information. Superpixel methods are indeed generally optimized and evaluated on noise-free natural color images, although specific tasks require to decompose highly textured or low resolution grayscale images, for instance in medical applications [21].

To overcome the limitations of handcrafted color spaces, deep learning approaches have been proposed [22, 23]. Nevertheless, the gain obtained with learned features on a training dataset comes at the expense of usual deep learning limitations, *i.e.*, important learning time, need for a substantial training database, and direct applicability limited to similar images. Moreover, these approaches do not directly extend to supervoxels and prevent from setting the shape regularity, which can highly impact the performances of superpixel-based tasks. It is thus still necessary to increase the robustness of non-deep learning superpixel methods to textures, while preserving their desired properties: adaptability, low complexity and limited parameter settings.

**Contributions.** In this work, we propose a new Texture-Aware SuperPixel (TASP) clustering method able to produce an accurate segmentation on any input image, from natural color to highly textured grayscale images.

TASP automatically adjusts the regularity constraint, according to the superpixel feature variance. In most recent methods, this parameter has to be globally set according to the image nature, and default or sub-optimal settings may highly impact the results [24]. Hence, TASP generates relevant superpixels regardless of the image content (see Figure 1), and addresses the need for fine manual regularity setting.

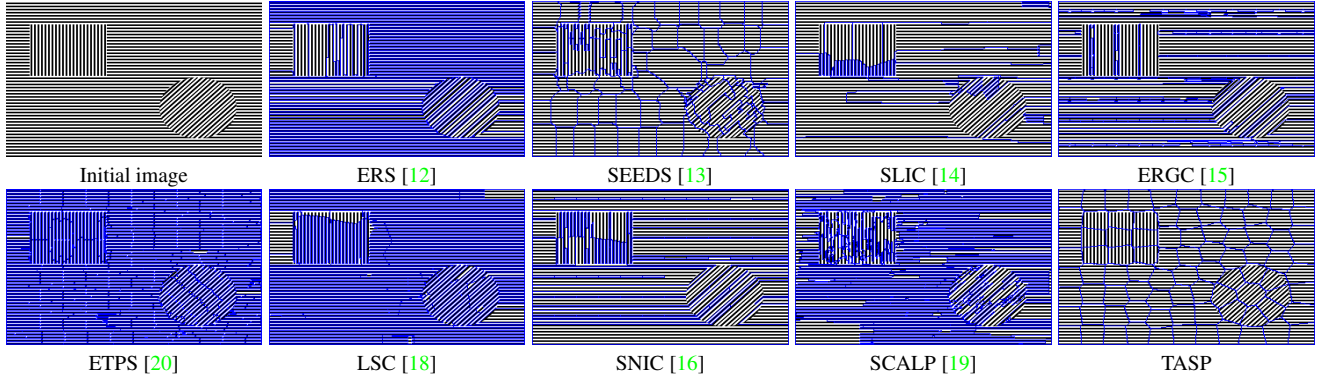


**Fig. 1.** Comparison of the proposed superpixel method TASP to state-of-the-art approaches on a synthetic example for  $K=90$ . Only TASP succeeds in detecting the textures while other methods are highly misled by contrast variations.

We also introduce a new patch-based distance term evaluating the texture compliance of a pixel to a superpixel, to ensure texture homogeneity within regions.

We validate TASP on natural color images from a standard segmentation dataset [25], and on two new image datasets proposed to evaluate texture segmentation performances. TASP substantially outperforms the state-of-the-art methods on texture segmentation performances, while performing as well, or better, on natural images, using the same parameters.

## 2. TEXTURE-AWARE SUPERPIXELS

The TASP method improves the SLIC [14] superpixel decomposition approach, that is first presented in this section. Then, we propose a method to locally set the spatial regularity parameter of superpixels, in order to automatically adapt to the image content. Finally, we introduce a new pixel to region texture homogeneity term to group pixels in terms of texture.

### 2.1. K-means-based Iterative Clustering

The standard framework of SLIC [14] only requires the number of superpixels to produce and a regularity parameter. The algorithm is based on an iteratively constrained K-means clustering of pixels. Superpixels  $S_i$  are first regularly set over the image domain as blocks of size  $s \times s$ , and are described by their average intensity feature  $F_{S_i}$  (CIE Lab colors for [14]) and their spatial barycenter  $X_{S_i} = [x_i, y_i]$  of pixels in  $S_i$ . The clustering relies on a feature  $d_F(F_p, F_{S_i}) = \|F_p - F_{S_i}\|_2$ , and a spatial distance term  $d_s(X_p, X_{S_i}) = \|X_p - X_{S_i}\|_2$ . At each iteration, each superpixel  $S_i$  is compared to all pixels  $p$ , of feature  $F_p$  at position  $X_p$ , within a  $(2s+1) \times (2s+1)$  region around its barycenter  $X_{S_i}$ . A pixel  $p$  is associated to the superpixel  $S_i$  minimizing the distance  $D$  defined as:

$$D(p, S_i) = d_F(F_p, F_{S_i}) + d_s(X_p, X_{S_i}) \frac{m^2}{s^2}, \quad (1)$$

where  $m$  is the parameter monitoring the superpixel shape regularity. Although this method accurately gathers pixels having similar colors,  $m$  is globally set and cannot adapt to all local image contours. It also highly fails to capture texture patterns, as it only considers color information at pixel level.

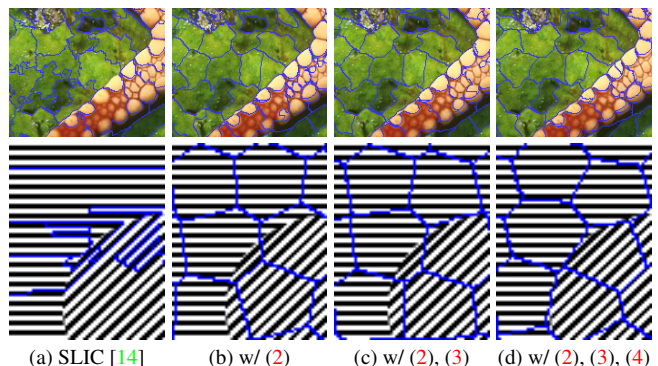


**Fig. 2.** SLIC [14] with optimal regularity for color images (a) vs TASP contributions (b)-(d), that accurately decomposes both color and texture images with the same parameters.

### 2.2. Local Adaptation of Superpixel Regularity

For most methods, *e.g.*, [14, 18, 19], the regularity parameter  $m$  must be manually set, according to the dynamic of the feature term  $d_F$ . Hence, default parameters for natural color images may lead model (1) to generate highly irregular clustering on textures, and the post-processing step enforcing connectivity to irreverently merge regions (see Figure 1). We address this issue by automatically weighting the regularity for each superpixel  $S_i$  according to the intensity variance in the feature space  $\sigma_i(F_p)$  of pixels  $p \in S_i$  such that:

$$m_{S_i} = m \exp\left(\frac{\sigma_i(F_p)^2}{\beta}\right), \quad (2)$$

such that the parameter  $\beta$  is able to increase the regularity constraint for superpixels having high feature variances. It also reduces the weight of  $d_s$  in smooth areas, so the superpixel boundaries can capture image objects that are perceptible from limited feature variations.

This way, without manually adapting  $m$  in (1), TASP can compute relevant superpixels on both natural color images (Figure 2(b)-top), and highly textured ones (Figure 2(b)-bottom), since (2) automatically adjusts the trade-off between  $d_F$  and  $d_s$  in (1). Nevertheless, the clustering accuracy can still be improved by using texture information.

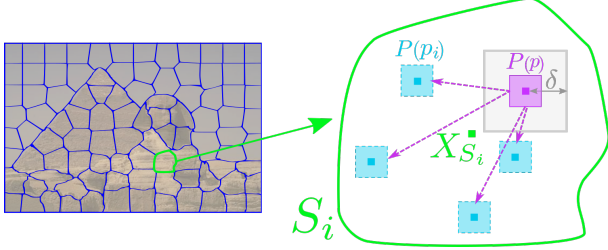


**Fig. 3.** Selection of similar patches  $P(p_i)$  in a superpixel  $S_i$  of barycenter  $X_{S_i}$ , outside a  $\delta$ -neighborhood, to compute the texture homogeneity term (3) for a patch  $P(p)$ .

## 2.3. Texture Homogeneity Measure

### 2.3.1. Pixel to Superpixel Patch-based Distance

In this section, we introduce in the clustering framework a new texture homogeneity term to gather pixels having similar colors but also similar local texture properties. The issue is to measure the similarity between the texture of a pixel neighborhood and the texture contained into a superpixel. The comparison is thus made between two regions of different sizes, and the texture information cannot be preserved with an average over the superpixel as for color and spatial information. Moreover, the framework complexity must remain limited, and able to adapt to any image content without any prior information. Such constraints prevent from using costly dictionary or learning-based approaches.

To address these issues, we propose a new pixel to superpixel texture homogeneity term using patch-based distances. For a pixel  $p$ , of patch  $P(p)$ , and a superpixel  $S_i$ , a nearest neighbor algorithm (see section 2.3.2) is used to find similar patches  $P(p_i)$  such that  $p_i \in S_i$ , and outside a  $\delta$ -neighborhood around  $p$  (see Figure 3). The new term  $d_P$  computes the average distance to the selected  $p_i \in S_i$ :

$$d_P(p, S_i) = \frac{1}{N} \sum_{p_i \in \mathcal{K}_p} d_P(p, p_i), \quad (3)$$

with  $\mathcal{K}_p$  the set of  $N$  selected pixels  $p_i \in S_i$ , compared with a patch distance in the feature space such that:  $d_P(p, p_i) = \frac{1}{n} \|F_{P(p)} - F_{P(p_i)}\|_2$ , with  $n$  the patch size.

This way, we can easily evaluate the texture compliance of a pixel to a superpixel, while leveraging the need for complex texture classification approaches.

### 2.3.2. Patch-based Nearest Neighbor Search

The search for similar patches can be performed by any  $k$ -nearest neighbor (NN) method. We choose to use Patch-Match, a fast iterative approximate-NN algorithm based on the propagation of good matches from adjacent neighbors [26]. The computation of  $d_P(p, S_i)$  can be directly performed for all pixels  $p$  in the  $(2s+1) \times (2s+1)$  area around the barycenter  $X_{S_i}$  of  $S_i$ . The algorithm being partly random,  $N$  patches in  $S_i$  can be selected in parallel for each pixel  $p$ , to increase the robustness of the texture homogeneity term (3).

### 2.3.3. Texture Unicity within Superpixels

In the texture term (3), the patch similarity is computed regardless of any spatial information. Hence, a pixel  $p$  to cluster may find similar local textures in restricted areas, leading a superpixel to potentially group several textures (Figure 2(c)).

To ensure the texture unicity within a superpixel  $S_i$ , we consider in (3) the spatial distance between the selected patches  $P(p_i)$ , at position  $X_{p_i} \in S_i$ , and  $X_{S_i}$ , the spatial barycenter of the superpixel  $S_i$  such that:

$$d_P(p, p_i) = \frac{1}{n} \|F_{P(p)} - F_{P(p_i)}\|_2 + \frac{m_{S_i}^2}{s^2} \Gamma(X_{p_i}, X_{S_i}), \quad (4)$$

with  $\Gamma$ , a scaling function defined such that  $\Gamma(X_{p_i}, X_{S_i}) = 2s^2(1 - \exp(-\|X_{p_i} - X_{S_i}\|_2^2/s^2))$ . Such term iteratively contributes to restrict the search area and the diversity of textures within the superpixel by highly penalizing similar patches found far from  $X_{S_i}$  (see Figure 2(d)). Hence, the barycenter is encouraged to move to a homogeneous textured area and to be contained within the superpixel, increasing the shape regularity, which is a desirable property [24].

Finally, the clustering distance in TASP is computed as:

$$D(p, S_i) = d_F(F_p, F_{S_i}) + d_s(X_p, X_{S_i}) \frac{m_{S_i}^2}{s^2} + d_P(p, S_i). \quad (5)$$

This way, TASP becomes a general decomposition method, efficient on various image types with the exact same parameters, as demonstrated in the next section.

## 3. RESULTS

### 3.1. Validation Framework

Similarly to [27], we create two new datasets to evaluate texture segmentation performances. A highly challenging synthetic stripe (mix-Stripes) dataset of 10 images of  $300 \times 400$  pixels, is created by putting stripes similar to the ones in Figure 1, in variable shaped regions of minimum size 1000 pixels. Natural textures with normalized intensity are also taken from the Brodatz dataset [28], to create 100 composite images (mix-Brodatz), that can contain up to 10 different textures. Finally, we consider the standard Berkeley Segmentation Dataset (BSD) [25], containing 200 natural color test images of size  $321 \times 481$  pixels.

Most parameters are empirically set once and for all, and their tuning has a very moderate impact on performances. For the patch search,  $N = 8$  patches of size  $5 \times 5$  pixels are selected outside a  $\delta = 3$  neighborhood. In the clustering model,  $m$  is set to 0.1 and  $\beta$  to 25 in (2), and the color features of [19] are used as features  $F$ . Finally, the whole clustering process of TASP is performed in 10 iterations as in [14].

TASP is compared to the recent state-of-the-art methods SLIC [14], ERGC [15], ETPS [20], LSC [18], SNIC [16], and SCALP [19]. Performances are evaluated with standard Achievable Segmentation Accuracy (ASA), and contour detection metric F-measure (F), as defined in [24].



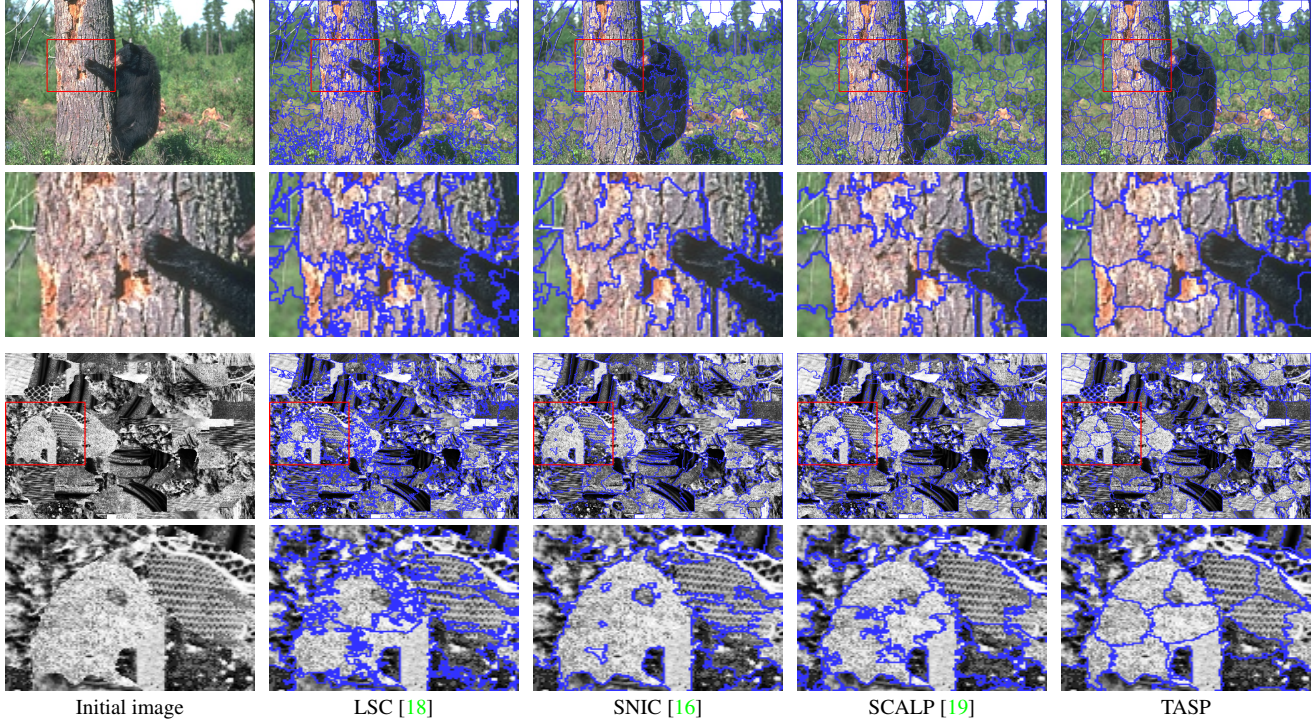


**Fig. 4.** Qualitative comparison between TASP and the state-of-the-art methods. TASP produces a more relevant result on an example image from mix-Brodatz (top), while performing as well or better, on a natural color image from the BSD (bottom).

### 3.2. Influence of Contributions

The impact of contributions is shown in Figure 2, and ASA and F measures are reported in Table 1 on the three datasets for  $K=250$  superpixels. Our new texture homogeneity term (3) and constraint of texture unicity within superpixels (4) both significantly improve performances on each data types.

Method	mix-Stripes		mix-Brodatz		BSD	
	ASA	F	ASA	F	ASA	F
TASP w/o (3),(4)	0.8303	0.3498	0.7969	0.4736	0.9484	0.4945
TASP w/o (4)	0.8486	0.3882	0.8112	0.4812	0.9493	0.4961
<b>TASP</b>	<b>0.8706</b>	<b>0.4232</b>	<b>0.8139</b>	<b>0.4824</b>	<b>0.9503</b>	<b>0.4992</b>

**Table 1.** Influence of the contributions in the TASP method.

### 3.3. Comparison to State-of-the-Art Methods

TASP is compared to the state-of-the-art methods on an image similar to the mix-Stripes dataset in Figure 1, and to the most recent ones on a mix-Brodatz and BSD image in Figure 4.

A quantitative evaluation is also performed on the three considered datasets in Table 2. TASP substantially increases the performances on the synthetic (mix-Stripes) and natural (mix-Brodatz) texture datasets, demonstrating its ability to provide texture-aware superpixels. TASP also outperforms the other methods on natural color images (BSD), using the same parameters, while other methods fail at providing accurate results on the three datasets at the same time. Finally, note that compared methods are used with parameters recommended by the authors. Nevertheless, no other approach

is able to capture texture information, so TASP with default parameters still outperform all compared methods manually optimized for each dataset.

Method	mix-Stripes		mix-Brodatz		BSD	
	ASA	F	ASA	F	ASA	F
SLIC [14]	0.7256	<u>0.4048</u>	0.7784	0.4607	0.9445	0.4706
ERGC [15]	0.6107	0.3717	0.7796	0.4677	0.9477	0.4571
ETPS [20]	<u>0.7769</u>	0.2953	0.7568	0.4354	0.9433	0.4710
LSC [18]	0.6979	0.3156	0.7908	0.4552	<u>0.9503</u>	0.4421
SNIC [16]	0.6659	0.3529	0.7662	<u>0.4815</u>	0.9410	0.4617
SCALP [19]	0.7307	0.3290	<u>0.7977</u>	0.4759	0.9499	<u>0.4914</u>
<b>TASP</b>	<b>0.8706</b>	<b>0.4232</b>	<b>0.8139</b>	<b>0.4824</b>	<b>0.9503</b>	<b>0.4992</b>

**Table 2.** TASP vs the state-of-the-art methods ( $K = 250$ ). Best and second results are respectively bold and underlined.

## 4. CONCLUSION

In this paper, we address the severe non-robustness of superpixel approaches to texture images by proposing a texture-aware decomposition method. A new patch-based distance is introduced to gather pixels having both similar color and local textural properties. The proposed method is general since it removes the need for manual setting of regularity constraint.

We outperform the segmentation of state-of-the-art methods on color, and synthetic and natural texture datasets, by using the exact same parameters. These results open the way for larger superpixel use and efficient application of our approach to medical image segmentation or video object tracking.

## 5. REFERENCES

- [1] Z. Liu, X. Zhang, S. Luo, and O. Le Meur, "Superpixel-based spatiotemporal saliency detection," *TCSVT*, vol. 24, no. 9, pp. 1522–1540, 2014. [1](#)
- [2] S. He, R. W. Lau, W. Liu, Z. Huang, and Q. Yang, "SuperCNN: A superpixelwise convolutional neural network for salient object detection," *IJCV*, vol. 115, no. 3, pp. 330–344, 2015. [1](#)
- [3] R. Sawhney, F. Li, and H. I. Christensen, "GASP: Geometric association with surface patches," in *3DV*, pp. 107–114, 2014. [1](#)
- [4] S. Gould, J. Zhao, X. He, and Y. Zhang, "Superpixel graph label transfer with learned distance metric," in *ECCV*, pp. 632–647, 2014. [1](#)
- [5] R. Gadde, V. Jampani, M. Kiefel, D. Kappler, and P. V. Gehler, "Superpixel convolutional networks using bilateral inceptions," in *ECCV*, pp. 597–613, 2016. [1](#)
- [6] R. Giraud, V.-T. Ta, A. Bugeau, P. Coupé, and N. Papadakis, "SuperPatchMatch: An algorithm for robust correspondences using superpixel patches," *TIP*, vol. 26, no. 8, pp. 4068–4078, 2017. [1](#)
- [7] P. Arbelaez, M. Maire, C. Fowlkes, and J. Malik, "Contour detection and hierarchical image segmentation," vol. 33, no. 5, pp. 898–916, 2011. [1](#)
- [8] G. Shu, A. Dehghan, and M. Shah, "Improving an object detector and extracting regions using superpixels," in *CVPR*, pp. 3721–3727, 2013. [1](#)
- [9] J. Yan, Y. Yu, X. Zhu, Z. Lei, and S. Z. Li, "Object detection by labeling superpixels," in *CVPR*, pp. 5107–5116, 2015. [1](#)
- [10] J. Chang, D. Wei, and J. W. Fisher, "A video representation using temporal superpixels," in *CVPR*, pp. 2051–2058, 2013. [1](#)
- [11] M. Reso, J. Jachalsky, B. Rosenhahn, and J. Ostermann, "Temporally consistent superpixels," in *ICCV*, pp. 385–392, 2013. [1](#)
- [12] M.-Y. Liu, O. Tuzel, S. Ramalingam, and R. Chellappa, "Entropy rate superpixel segmentation," in *CVPR*, pp. 2097–2104, 2011. [1, 2](#)
- [13] M. Van den Bergh, X. Boix, G. Roig, B. de Capitani, and L. Van Gool, "SEEDS: Superpixels extracted via energy-driven sampling," in *ECCV*, pp. 13–26, 2012. [1, 2](#)
- [14] R. Achanta, A. Shaji, K. Smith, A. Lucchi, P. Fua, and S. Süsstrunk, "SLIC superpixels compared to state-of-the-art superpixel methods," *PAMI*, vol. 34, pp. 2274–2282, 2012. [1, 2, 3, 4](#)
- [15] P. Buysens, I. Gardin, S. Ruan, and A. Elmoataz, "Eikonal-based region growing for efficient clustering," *IVC*, vol. 32, no. 12, pp. 1045–1054, 2014. [1, 2, 3, 4](#)
- [16] R. Achanta and S. Süsstrunk, "Superpixels and polygons using simple non-iterative clustering," in *CVPR*, pp. 4895–4904, 2017. [1, 2, 3, 4](#)
- [17] Y.-J. Liu, C.-C. Yu, M.-J. Yu, and Y. He, "Manifold SLIC: A fast method to compute content-sensitive superpixels," in *CVPR*, pp. 651–659, 2016. [1](#)
- [18] J. Chen, Z. Li, and B. Huang, "Linear spectral clustering superpixel," *TIP*, vol. 26, pp. 3317–3330, 2017. [1, 2, 3, 4](#)
- [19] R. Giraud, V.-T. Ta, and N. Papadakis, "Robust superpixels using color and contour features along linear path," *CVIU*, vol. 170, pp. 1–13, 2018. [1, 2, 3, 4](#)
- [20] J. Yao, M. Boben, S. Fidler, and R. Urtasun, "Real-time coarse-to-fine topologically preserving segmentation," in *CVPR*, pp. 2947–2955, 2015. [1, 2, 3, 4](#)
- [21] Z. Tian, L. Liu, Z. Zhang, and B. Fei, "Superpixel-based segmentation for 3D prostate MR images," *TMI*, vol. 35, no. 3, pp. 791–801, 2016. [1](#)
- [22] V. Jampani, D. Sun, M.-Y. Liu, M.-H. Yang, and J. Kautz, "Superpixel sampling networks," in *ECCV*, 2018. [1](#)
- [23] W.-C. Tu, M.-Y. Liu, V. Jampani, D. Sun, S.-Y. Chien, M.-H. Yang, and K. Jan, "Learning superpixels with segmentation-aware affinity loss," in *CVPR*, 2018. [1](#)
- [24] R. Giraud, V.-T. Ta, and N. Papadakis, "Evaluation framework of superpixel methods with a global regularity measure," *JEI*, vol. 26, no. 6, 2017. [1, 3](#)
- [25] D. R. Martin, C. C. Fowlkes, and J. Malik, "Learning to detect natural image boundaries using local brightness, color, and texture cues," *PAMI*, vol. 26, no. 5, pp. 530–549, 2004. [2, 3](#)
- [26] C. Barnes, E. Shechtman, A. Finkelstein, and D. B. Goldman, "PatchMatch: A randomized correspondence algorithm for structural image editing," *ToG*, vol. 28, no. 3, 2009. [3](#)
- [27] T. Randen and J. H. Husoy, "Filtering for texture classification: A comparative study," *PAMI*, vol. 21, no. 4, pp. 291–310, 1999. [3](#)

[28] P. Brodatz, "Textures: A photographic album for artists and designers," *Dover Publications*, 1966. 3